Available online at www.sciencedirect.com
SCIENCE DIRECT®
European Journal of Medicinal Chemistry 40 (2005) 1134–1142
EUROPEAN JOURNAL OF MEDICINAL CHEMISTRY
www.elsevier.com/locate/ejmech

Original article

AMBER force field implementation of the boronate function to simulate the inhibition of β-lactamases by alkyl and aryl boronic acids

Andrea Tafi [a], Mariangela Agamennone [b], Paolo Tortorella [c], Stefano Alcaro [d], Carlo Gallina [b], Maurizio Botta [a,*]

[a] *Dipartimento Farmaco-Chimico-Tecnologico, Università degli Studi di Siena, Via Aldo Moro, I-53100 Siena, Italy*
[b] *Dipartimento di Scienze del Farmaco, Università "G. d'Annunzio" di Chieti, Via dei Vestini 31, 66013 Chieti, Italy*
[c] *Dipartimento Farmaco-Chimico, Università degli Studi di Bari, Via Orabona 4, 70125 Bari, Italy*
[d] *Dipartimento di Scienza Farmacologiche, Università degli Studi di Catanzaro, Complesso Ninì Barbieri, 88021 Roccelletta di Borgia, Catanzaro, Italy*

Received 21 July 2004; received in revised form 28 April 2005; accepted 15 June 2005

Available online 08 September 2005

Abstract

Boronic acids are a very appealing class of serine proteases inhibitors whose rational design suffers, in spite of their therapeutic potential, from the lack of boron-related parameters in force fields commonly used for proteins. We introduced bonded, non-bonded and point charges in the MacroModel/Amber force field, as well as GB/SA solvation parameters, to model boronic acids as tetrahedral adducts formed after protease's serine Oγ coordination. With the aim to check the implemented force field, flexible docking studies were performed on three crystallographic complexes of β-lactamases with boronic acids that output the crystallographic conformation of the complexes as the global minimum energy structure. Although the used approach was basic, nevertheless the resultant force field seems to be efficient and suitable for the structure-based design of new boronic inhibitors of β-lactamases.

Keywords: Amber; Boronic acid; Force field parameterization; β-Lactamases

1. Introduction

β-Lactamases are important therapeutic targets because they mediate the major resistance mechanism against β-lactam antibiotics, such as penicillin and cephalosporin. β-Lactam agents that inhibit these enzymes, such as clavulanic acid [1] and compounds less susceptible to enzyme hydrolysis, such as monobactams, have been widely used in antibiotic therapy to overcome the action of β-lactamases. The similarity of these compounds to the drugs they are meant to protect or replace has allowed bacteria to evolve further, maintaining their resistance. One way to avoid falling into this resistance mechanism again would be to develop inhibitors structurally dissimilar to β-lactams.

Boron containing compounds are of increasing interest in the medicinal chemistry field [2, 3]. Only few natural products containing boron are known, since nature lacks biosynthetic pathways to form a boron–carbon bond and it might probably lack metabolic enzymes able to break it down. This circumstance would represent an advantage if these molecules were employed as therapeutic agents. Among the different organic compounds containing boron, boronic acids $RB(OH)_2$ are particularly suited for drug design owing to their low toxicity, adequate stability under physiological conditions, and practically neutral behavior [3]. Boronic acids, moreover, owing to their strong Lewis acid character, can readily interconvert from the trigonal, planar sp^2 form to anionic, tetrahedral, sp^3 complexes, by coordination of various nucleophiles. Thus, properly designed boronic acids have been shown to form very tight complexes with several serine proteases such as chymotrypsin, β-lactamases, trypsin and thrombin (see Scheme 1).

Abbreviations: GB/SA, generalized Born surface area; MCMM, Monte Carlo multiple minimum; MM/MD, molecular mechanics/molecular dynamics; PDB, protein data bank; RMSD, root mean square distance; TNCG, truncated Newton conjugate gradient.

* Corresponding author. Tel.: +39 0577 234 306; fax: +39 0577 234 333.
E-mail address: botta@unisi.it (M. Botta).

0223-5234/$ - see front matter © 2005 Elsevier SAS. All rights reserved.
doi:10.1016/j.ejmech.2005.06.011

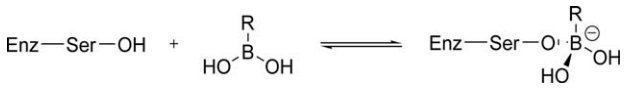

Scheme 1.

Boronic acids, as proteases inhibitors, appeared for the first time 30 years ago as chymotrypsin [4] and β-lactamase inhibitors [5]. Since then, interest in these molecules increased continuously and boronic acids with nanomolar affinity for β-lactamases have been published [6] and patented [7] recently.

Tem-1 is the most widespread β-lactamase and aminoacid substitutions are frequently encountered in clinical variants of this enzyme that are able to hydrolyze third generation cephalosporins and monobactams [8]. Being presently interested in finding new boronic inhibitors against class A β-lactamases like Tem-1 [9], we embarked in advance in the modeling of the inhibition of Tem-1 and of other serine β-lactamases by alkyl and aryl boronic acids, employing the software MacroModel [10] implemented with the AMBER* united atom force field [11–13]. X-ray crystal structures show that boronic acids inhibit β-lactamases by the formation of tetrahedral adducts, analogous to the deacylation tetrahedral intermediate of these enzymes [14,15]. Similarly to other authors [16], therefore, we focused our attention on the interactions between inhibitors and enzymes as tetrahedral adducts formed after catalytic serine Oγ coordination, neglecting, for now, the influence of the recognition step, leading to the formation of the Michaelis–Menten complex.

Boron-related parameters, however, useful to mimic the tetrahedral boronate functional group embedded in a protein environment and exploitable in commonly used software packages, have not been developed until now. To get around this difficulty, some authors have modeled alkyl boronic acids as serine protease inhibitors with TRIPOS force field after substituting the boron atom with a carbon [17,18] and correcting the bond lengths involving boron on the basis of crystallographic data [16,19]. Such an approximation, however, even though suitable for the application of a pure "docking" methodology, seems too simple for a MM/MD approach that needs all force field parameters to accurately simulate conformational flexibility.

The first example of boron parameter implementation dates back to 1987 when parameters for boron enolates as transition states were introduced in MM2 force field [20]; this parameterization was refined afterwards to include allyl and crotyl boronates in addition to aldehydes [21–23]. In 1996 further MM2 boron parameters were published [24] while trivalent alkylboronic acids were parameterized in OPLS [25]. The most complete parameterization for alkyl and aryl boronic acids, both as trivalent and tetrahedral adducts, has been recently implemented in CHARMM force field [26][1].

[1] In the study by Pletnev et al., stretching and bending interactions involving boron as the central atom have been modeled by application of the Gillespie–Kepert theory, so that the corresponding parameters are not exploitable in standard softwares such as MacroModel.

The relevance of the subject of our research and the lack of suitable parameters prompted us to tackle the implementation of the boronate function in AMBER*, introducing GB/SA boron solvation parameters as well. The new set of parameters was developed starting from literature, X-ray data, semi-empirical and ab initio calculations. We report here the results of our parameterization work together with some validation studies, in which the inhibition of Tem-1 and Amp-C β-lactamases by known boronic inhibitors were simulated.

2. Force field parameterization

The AMBER* force field is described by the following equation [11]:

$$V=\frac{1}{2}\sum_{bonds}\left(K_b\left(b-b_o\right)^2\right)+\frac{1}{2}\sum_{angles}\left(K_\theta\left(\theta-\theta_o\right)^2\right)+\frac{1}{2}\sum_{dihedrals}\left(K_\varphi\left(1+\cos\left[n\varphi-\gamma\right]\right)\right)+\sum_{nonbonded}\left[\frac{A}{r^{12}}-\frac{B}{r^6}\right]+\sum_{nonbonded}\frac{q_1q_2}{\epsilon r}+\sum_{H-bonds}\left[\frac{C}{r^{12}}-\frac{D}{r^6}\right] \quad (1)$$

The first three terms in Eq. (1) handle the internal coordinates of bond stretchings, angle bendings and torsions. The non-bonded terms account for the van der Waals and electrostatic interactions and the last term represent the 12-6 Lennard–Jones hydrogen bond treatment.

The force field parameterization was performed by introducing the non-bonded parameters for the boron atom in the Main Parameters section of the force field file (amber.fld) and adding two substructures for the tetrahedral adducts of alkyl and aryl boronic acids, in the Substructure section of the same file. These substructures were inserted as suggested in the MacroModel/Batchmin reference manual [27]. All the introduced parameters are shown in Tables 1–4.

2.1. Stretching, bending and torsional terms

Input stretching equilibrium distance values were obtained calculating the average length of the B–C and B–O bonds in the X-ray crystal complexes of boronic acids with serine proteases [14,15]. Semi-empirical geometry optimization calculations were carried out as well on standard structures **1** and **2** (see Scheme 2) with MOPAC/AM1 [28] to broaden the data set available from crystal structures. Stretching force constants were calculated from the average values of the IR stretching frequencies of the B–O (1345 cm^{-1}) and B–C (930 cm^{-1}) bonds [21], applying the equation suggested in MacroModel/Batchmin reference manual [27]:

$$K\,(stretch)=3.0\times10^{-5}\;\nu^2\;M_1M_2/(M_1+M_2) \quad (2)$$

where ν is the stretching IR frequency in wave numbers (cm^{-1}) and M_1 and M_2 are the atomic masses of the atoms involved in the stretch. The stretching equilibrium values

Table 1
Substructure introduced into the MacroModel/BatchMin amber.fld file (substructure section) and describing arylboronic acids

C	Arylboronate							
9	B3(–O3–H2)–O3–H2							
–2								
1	C2	1			1.6100	160.0000		
1	1	2			1.4900	350.0000		
1	1	4			1.4900	350.0000		
1	1	O3			1.6500	350.0000		
2	2	1	4		109.5000	60.0000		
2	2	1	O3		109.5000	60.0000		
2	4	1	O3		109.5000	60.0000		
2	C2	1	2		109.5000	35.0000		
2	C2	1	4		109.5000	35.0000		
2	C2	1	O3		109.5000	35.0000		
2	1	2	3		109.5000	35.0000		
2	1	4	5		109.5000	35.0000		
2	C2	C2	1		130.0000	70.0000		
2	1	O3	C3		113.0000	50.0000		
4	O3	1	C2	00	0.0000	0.0000	0.0000	
54					0.0000	0.0000	0.0200	
4	2	1	C2	00	0.0000	0.0000	0.0000	
54					0.0000	0.0000	–0.1000	
4	4	1	C2	00	0.0000	0.0000	0.0000	
54					0.0000	0.0000	–0.1000	
4	00	1	2	3	0.0000	0.0000	0.2000	
4	00	1	4	5	0.0000	0.0000	0.2000	
4	00	1	O3	C3	0.0000	0.0000	–0.1000	
4	00	C3	O3	1	0.0000	0.0000	0.0100	
–3								
C	Arylboronate charges							
9	C2–B3(–O3–H2)(–O3–H2)–O3–CB							
–4								
8	–0.3296	0.7827	–0.9081	0.4207	–0.8550	0.3735	–0.7014	0.2200

Table 2
Substructure introduced into the MacroModel/BatchMin amber.fld file (substructure section) and describing alkylboronic acids

C	Alkylboronate							
9	CA–B3–O3							
–2								
1	1	2			1.6300	340.0000		
1	2	3			1.5100	450.0000		
1	2	O3			1.5100	450.0000		
2	3	2	O3		109.5000	60.0000		
2	1	2	3		109.5000	40.0000		
2	1	2	O3		109.5000	40.0000		
2	2	3	H2		109.5000	35.0000		
2	2	O3	CB		113.0000	50.0000		
4	00	2	1	00	0.0000	0.0000	2.0000	
4	00	2	O3	CB–	0.0000	0.0000	0.1000	
4	00	2	3	H2	0.0000	0.0000	0.2000	
4	00	CB	O3	2	0.0000	0.0000	0.0100	
–3								
C	Alkylboronate charges							
9	CA–B3(–O3–H2)(–O3–H2)–O3–CB							
–4								
8	–0.4098	1.0377	–0.9163	0.3822	–0.7626	0.3745	–0.9260	0.2200

Table 3
Van der Waals parameters introduced into the Main Parameter Section of the MacroModel/BatchMin amber.fld file

C	Van der Waals Interactions (VDW)Opt. Descriptor				
C					
C	Radius	Epsilon	Offset	Charge	Atm1 Lp
C	(Å)	(Kcal mol–1)	(Å)	(Electrons)	
–6					
B3	1.9800	0.0340			0000 A2

were further adjusted through a trial-and-error procedure to obtain the best matching between experimental and MM data.

Both X-ray data and the results of our semi-empirical calculations pointed out displacements of the bendings involving boron as central atom out of the values expected for a tetrahedral geometry (109.5°). Since it was not possible to directly reproduce this structural detail in an unambiguous way, force constants for the bendings involving boron as central atom were taken from MM2 parameterization by Whiting et al. [24], after having multiplied these values for the conversion factor between MM2 and AMBER* [27], while their equilibrium values were set to 109.5°. The non–bonded interactions were expected to account for the experimentally observed deviations. All the others missing bending parameters not involving boron as the central atom were adopted from Pletnev et al. [26][1].

Torsion parameters were adopted from Pletnev et al. [26] to describe both alkyl and aryl boronic acids.

2.2. Electrostatic, van der Waals and solvation terms

ESP partial charges were computed by the HF method with 6-31G** basis set, using the program Jaguar [29]. Calculations were performed on **1** and **2** (see Section 5 for more details) and the new partial charges introduced in the substructure section of the amber.fld file (see Tables 1 and 2).

Van der Waals parameters (see Table 3) were taken from MM2 force field [20], implemented in MacroModel, as already suggested by Pletnev [26].

Since the active site of β-lactamases is solvent exposed and several residues of this cleft are polar, water effects were not negligible; they were therefore included in the docking studies according to the GB/SA Generalized Born Surface Area continuum solvation treatment [30]. Four boron solvation parameters had to be introduced in the water.slv file and they were assigned according to a quite simple and conservative procedure (see Table 4). The atomic radius of boron, taken from an OPLS parameterization [25], was used as the

Table 4
Parameters for boron introduced into the water.slv file

	SMODEL 3.00 GB/SA Solvation			
	RADIUS (Å)	ENERGY (kJ Å^{-2})	P TYPE (3 body ON)	P TYPE (3 body OFF)
ATM B3	2.0800E00	0.03000E0	1.0500000	1.3933470

1 **2**

Scheme 2.

van der Waals radius, in compliance with the general procedure applied in the derivation of the GB/SA method [30]. The energy parameter was set to 0.03 kJ Å^{-2}, that is, using the generalized parameter already assigned in MacroModel to C, P and all the metal ions (Li, Na, K, Rb, Cs, Ca, Ba) and, similarly, the two P type parameters were fixed assigning to boron the MacroModel generalized values of phosphorous, halogen atoms and metal ions.

2.3. Torsional profiles comparison

Ab initio torsional profiles were calculated on the simplified structures **1** and **2** and compared with the corresponding MM profiles. The overall torsional energy profile of a system, in fact, is greatly influenced by charges and van der Waals parameters of the atoms involved and consequently, mixing of parameters from different sources can be done if, in the final step, MM torsional profiles are verified to reproduce the corresponding quantum chemical potentials.

2.4. Test cases

Three crystal complexes of β-lactamases with boronic acids were downloaded from the Brookhaven Protein Data Bank as an experimental reference (PDB entries: 1erm, 1ero and 1kds) to test the capability of our customized force field to reproduce the experimental structure of the inhibited enzymes and to define a reliable modeling protocol to be applied to the design of new boronic inhibitors [31]. Structures 1erm and 1ero show Tem-1 inhibited by two alkyl boronic acids {(*R*)1-acetamido-2-(3-carboxyphenyl)ethaneboronic acid **3** [14] and (*R*)1-phenylacetamido-2-(3-carboxyphenyl)ethaneboronic acid **4** [14], respectively} while structure 1kds describes Amp-C inhibited by an aryl boronic acid (3-nitrophenylboronic acid **5** [15]) (see Scheme 3). A minimization of the complexes was firstly performed. Flexible docking studies were undertaken afterwards (see Section 5 for detailed explanations), in which the outcome of the second step of the inhibition reaction—leading to the formation of the tetrahedral adducts—was simulated. Accordingly, Monte Carlo MCMM searches were accomplished on 1erm, 1ero and 1kds, applying a broadly experimented procedure [31,32]. Crystal water molecules were not included in the calculations. In the case of 1erm and 1kds further docking experiments were rerun retaining a few water molecules directly involved in interactions between inhibitor and enzyme[2].

[2] In the crystal structure 1ero no water molecules were retained as none of them was detected within 4.0 Å from the inhibitor.

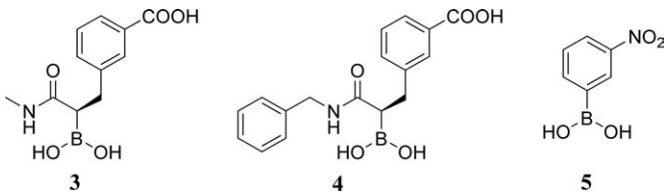

Scheme 3.

The fitting between each crystal complex and the respective modeled structure was evaluated by calculating the root mean square distance (RMSD) between corresponding pairs of atoms.

3. Results and discussion

The results of the torsional profiles comparison performed on **1** and **2** are shown in Fig. 1. The good level of correlation displayed in the figure between ab initio and MM energy profiles gave evidence of the reliability of the performed parameterization.

Minimizations carried out on the three crystal complexes mentioned above gave the results summarized in Table 5. RMSD values calculated superimposing the minimized subset (see Section 5 for the subset definition) of each complex with the corresponding X-ray reference were in the range between 0.58 and 1.12 Å. The minimum and maximum RMSD values lowered to 0.18 and 0.45, respectively, when solely the inhibitor was taken into account, showing the suitable quality of the introduced parameters. Notably, in the case of 1erm, the full deletion of crystal water molecules affected the result of the minimizations while, on the contrary, the same action performed on 1kds did not induce a similar displacement of the inhibitor, making the match between the experimental complex and the computationally optimized structure better.

The results of the simulations concerning the second step of the inhibition process of Tem-1 and Amp-C by boronic inhibitors were satisfactory as well, as shown by the RMSDs reported in Table 6, resulting from the superimposition of each calculated global minimum and the corresponding X-ray geometry. The superimposition between calculated and experimental structures, are shown in Figs. 2–4. Both the applied procedures (without crystal water molecules and with the relevant ones) were able to identify the experimental X-ray structures among the theoretical lowest energy poses. Moreover, the calculated global minimum geometry was found to correspond to the experimental crystallographic 1erm and 1kds structures, in the simulations performed including crystal water molecules.

The results of our docking studies highlighted the important role played by ordered water molecules in stabilizing the global minimum pose. In the case of 1erm complex (shown in Fig. 2A), for instance, the carboxylate of the inhibitor was stabilized by WAT304 bridging the gap between this functional group and residues Arg243 and Val216 by hydrogen bonding interactions, significantly stabilizing the enzyme–inhibitor interaction. WAT341, as well, connected in a network with other water molecules, was found to link (through H-bonds) the acetamide carbonyl oxygen of the inhibitor with Glu166, allowing the acetamide NH to interact with the carbonyl oxygen of Ala237. In the lowest energy output structure obtained without crystal water molecules, differently (see Fig. 2B), the acetamide chain was found to be rotated of about 90°, with respect to the crystallographic structure, so to form a direct hydrogen bond with NH_2 of Asn132, while, the carboxylic group retained its strong interactions with a region of the active site characterized by some polar positively charged residues. As a matter of fact, in the docking performed without water molecules, the crystallographic pose was observed at 17.1 kJ mol^{-1} over the global minimum (RMSD inhibitor 0.68).

In the case of the 1kds complex (shown in Fig. 3) water seemed to have a relevant role as well: WAT401, for instance,

Table 5
Root mean square distance values (RMSD) obtained superimposing each minimized structure (with and without crystal water molecules) with the corresponding X-ray crystal structure

Complex	RMSD (minimized subset[a])	RMSD (inhibitor)
1erm Water	0.59[b]	0.18
1erm No Water	0.71[c]	0.31
1kds Water	1.11[d]	0.36
1kds No Water	1.12[e]	0.23
1ero	0.58[f]	0.45

[a] See Section 5 for the subset definition.
[b] 165 atoms superimposed out of the total number of 2620 atoms.
[c] 150 atoms superimposed out of the total number of 2605 atoms.
[d] 155 atoms superimposed out of the total number of 3493 atoms.
[e] 149 atoms superimposed out of the total number of 3487 atoms.
[f] 130 atoms superimposed out of the total number of 2614 atoms.

Table 6
Root mean square distance values (RMSD) obtained superimposing the global minimum geometry resulting from docking experiments (with and without crystal water molecules) with the corresponding X-ray crystal structure

Complex	RMSD (minimized subset[a])	RMSD (inhibitor)
1erm Water	0.96[b]	0.65
1erm No Water	1.08[c]	1.09
1kds Water	1.26[d]	0.71
1kds No Water	1.88[e]	1.83
1ero	1.80[f]	2.10

[a] See Section 5 for the subset definition.
[b] 165 atoms superimposed out of the total number of 2620 atoms.
[c] 150 atoms superimposed out of the total number of 2605 atoms.
[d] 155 atoms superimposed out of the total number of 3493 atoms.
[e] 149 atoms superimposed out of the total number of 3487 atoms.
[f] 130 atoms superimposed out of the total number of 2614 atoms.

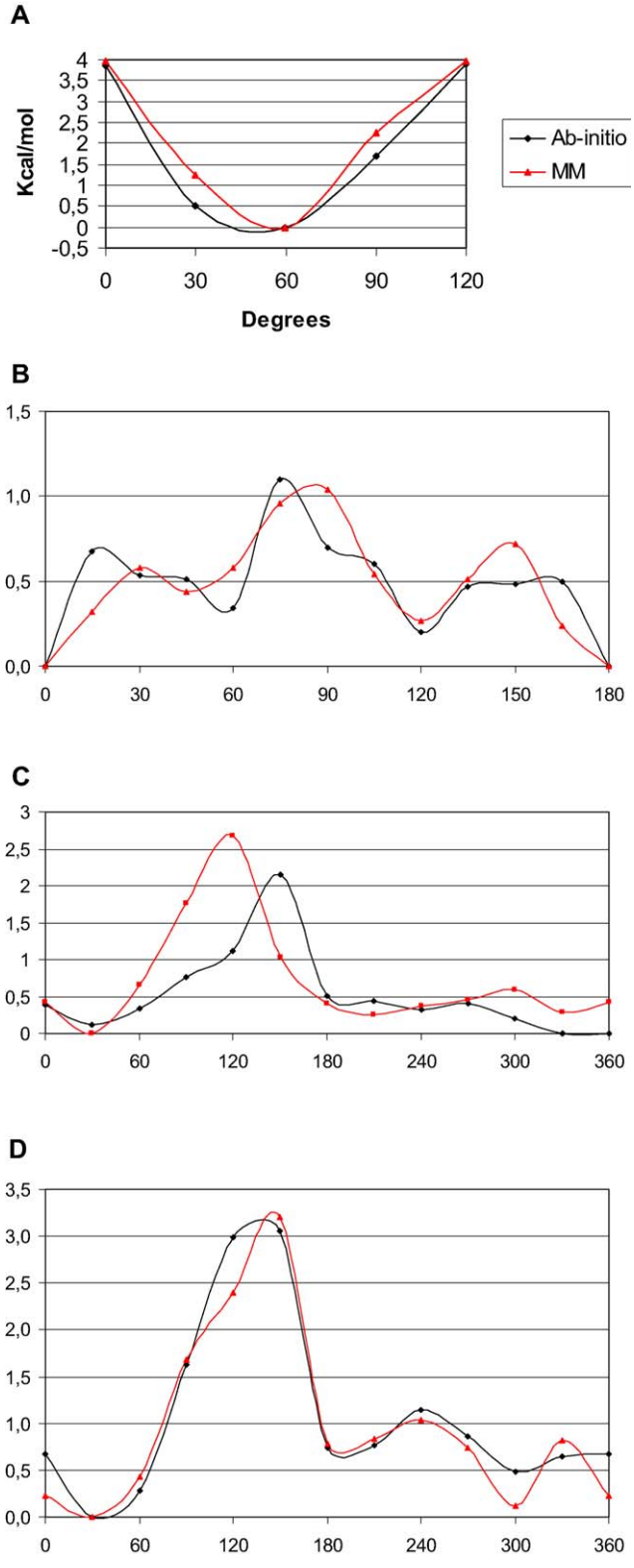

Fig. 1. Torsional profiles comparison between ab initio and MM calculations of, respectively: (**a**) torsion EtO–B–C–H evaluated for the alkylboronate **2**. The profile shows a periodicity of 120°, therefore only the corresponding portion of the energy contour has been calculated. (**b**) Torsion EtO–B–C–C evaluated for the arylboronate **1**. The profile shows a periodicity of 180°, therefore only the corresponding portion of the energy contour has been calculated. (**c**) Torsion EtO–B–O–H evaluated for the alkylboronate **2**. (**d**) Torsion Et–O–B–OH evaluated for the alkylboronate **2**.

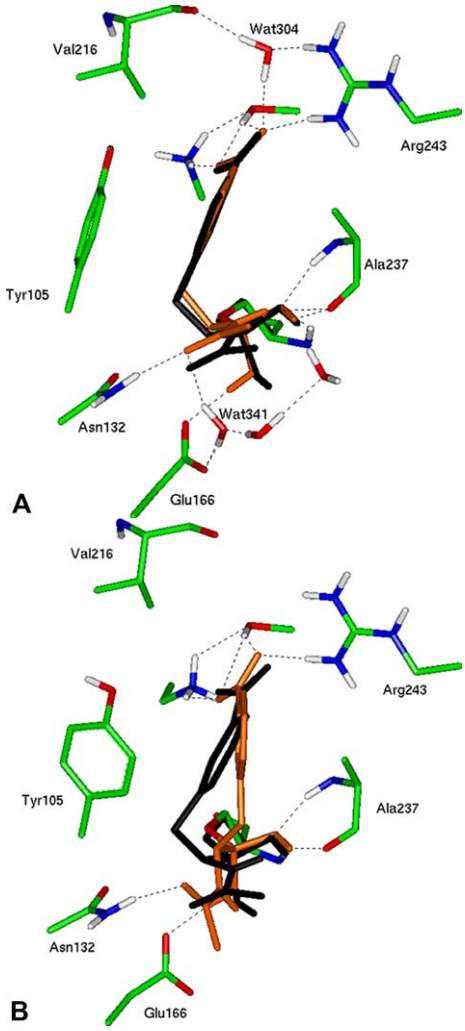

Fig. 2. [33] Superimposition between the calculated global minimum geometry of the adduct formed by Tem-1 (colored by atom types) with the inhibitor (*R*)1-acetamido-2-(3-carboxyphenyl)ethaneboronic acid (orange) and the crystallographic pose of the inhibitor (black) located at its proper 3D position inside the active site of the enzyme. Hydrogen atoms bound to heteroatoms are displayed. Hydrogen bonding interactions are depicted as dotted lines. In A, results obtained when relevant water molecules were included in the calculations are shown, whereas in B, the results obtained without water molecules are displayed. For the sake of simplicity, only residues discussed in the text are shown.

is shown in Fig. 3A to bind as a bridge the two hydroxyl groups of the boronate; the conformation adopted by the boronic function is consequently stabilized by seven hydrogen bonds (two with water and five with the surrounding residues), and promotes the stacking interaction of the phenyl ring with the Tyr221. In the docking without water molecules (see Fig. 3B), otherwise, the boronate is arranged to form a new hydrogen bond between the catalytic serine oxygen and Tyr150. Moreover, the aromatic moiety of the inhibitor overturns to establish a T-shaped aromatic interaction with the phenyl ring of Tyr150 and to enable the NO_2 to form a hydrogen bond with Asn289 (see Fig. 3B). Notably, also in the case of 1kds, the crystallographic conformation was found as pose

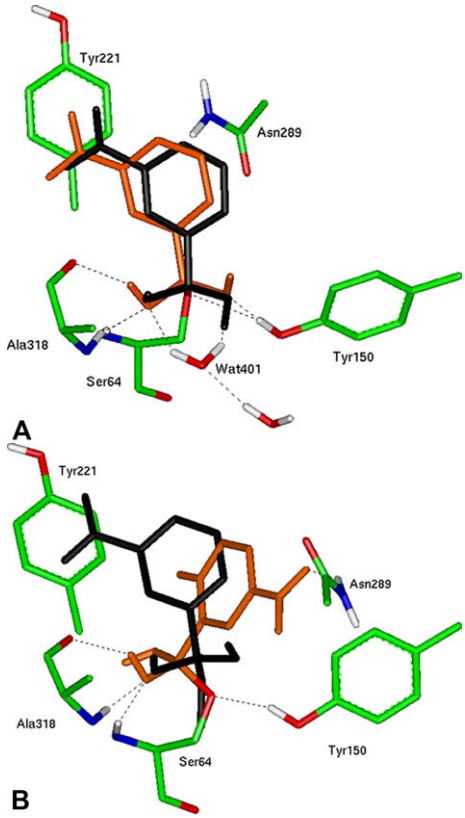

Fig. 3. [33] Superimposition between the global minimum geometry of the adduct formed by Amp-C (colored by atom types) with the inhibitor 3-nitrophenylboronic acid (orange) and the crystallographic pose of the inhibitor (black) located at its proper 3D position inside the active site of the enzyme. Hydrogen atoms bound to heteroatoms are displayed. Hydrogen bonding interactions are depicted as dotted lines. In A, the results obtained when relevant water molecules were included in the calculations are shown, whereas in B, the results obtained without water molecules are displayed. For the sake of simplicity, only residues discussed in the text are shown.

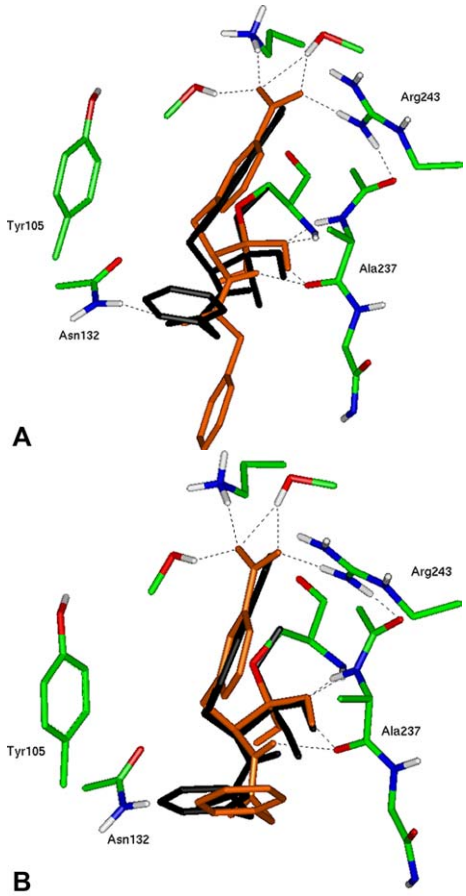

Fig. 4. [33] Superimposition between the calculated geometries of the adduct formed by Tem-1 (colored by atom types) with the inhibitor (*R*)1-phenylacetamido-2-(3-carboxyphenyl) ethaneboronic acid (orange) and the and the crystallographic pose of the inhibitor (black) located at its proper 3D position inside the active site of the enzyme. In A, the calculated global minimum geometry of the inhibitor is shown, whereas in B, the calculated pose more similar to the crystallographic conformation is displayed. Hydrogen atoms bound to heteroatoms are shown. Hydrogen bonding interactions are depicted as dotted lines. For the sake of simplicity only residues discussed in the text are shown.

number 17 at 17.4 kJ mol^{-1} above the global minimum (RMSD inhibitor 0.67).

In the case of 1ero, finally, interesting results were obtained as well. Two geometries of approximately equal occupancy have been described for this crystal [14], differing because of the position of the aromatic moiety, that adopts two alternative orientations. The first one, described by the PDB crystal structure and displayed in black in Fig. 4, shows a favorable aromatic T-shaped interaction between the two phenyl rings of the inhibitor, while in the second one the phenylacetamido group forms van der Waals interactions with the edge β-strand of the enzyme active site (residues 235–238). Our docking studies gave the second alternative conformation as the global minimum pose (displayed in orange in Fig. 4A superimposed to the crystal structure), as demonstrated by the distance values between O amide NH_2 Asn132 (3.4 Å) and NH amide O Ala237 (2.9 Å), comparable with the values described in the article (3.5 and 3.3 Å). Also in this case, anyhow, the conformation corresponding to the deposited crystal complex was found at 13.2 kJ mol^{-1} over the global minimum (RMSD inhibitor 0.67, RMSD minimized subset 0.95) and is displayed in Fig. 4B.

4. Conclusions

In the present work parameters for boronic acids were implemented in the force field AMBER*, with the aim to model boronic acids as β-lactamases inhibitors. A simple procedure was adopted to implement the force field, in which the parameters were mixed from a few sources. Although the approach was basic in this sense, nevertheless the new force field seemed to be efficient and reliable in reproducing the structure of the boronate function and suitable for our docking purposes, as demonstrated by the simulations performed on three reference crystal structures. Moreover, the applied docking procedure was sensitive enough to highlight the role of water molecules in determining the binding geometry. This issue, in a particular manner, constitutes an important problem of general interest and is not simply related to this parameterization work.

In sum, we propose that our parameter set may be considered a useful tool for the application of Amber* force field to the study of boronic acids in their inhibition process of serine proteases.

5. Experimental protocols

The software packages MacroModel/BatchMin 5.5 and 6.5 [10] equipped with the AMBER* united atom force field [11–13] were used for our calculations performed on SGI O2 R10000 and Origin 300 workstations.

Semi-empirical molecular orbital calculations were performed using the MOPAC 6.0 [28] module implemented in Insight II [34], applying the AM1 Hamiltonian [35] to optimize the simplified structures **1** and **2** (Scheme 2).

The charge derivation was carried out by the HF method with 6-31G** basis set, using the program Jaguar [29]. The optimization of the geometries of **1** and **2** was carried out with the same method until the default convergence criterion of the Jaguar input was reached.

The MM torsional profiles were calculated submitting structures **1** and **2** to "dihedral drive" calculations (command DRIV) using the MacroModel 5.5 software package. DRIV routine allows to rotate a specified dihedral angle and to optimize the structure at each step, keeping fixed the atomic coordinates of the four atoms defining that torsion. Four types of dihedral angle were taken into account, corresponding to the four typologies involving boron as one of the central atoms: EtO–B–C–H, Et–O–B–OH, EtO–B–O–H for the alkylboronate **2** and EtO–B–C–C for the arylboronate **1**. They were rotated from 0° to, respectively, 120° (increment 30°), 360° (increment 30°), 360° (increment 30°) and 180° (increment 15°). Minimizations were finished at a derivative convergence of 10^{-3} kJ $Å^{-1}$ mol^{-1} using the Truncated Newton Conjugate Gradient (TNCG) algorithm. The ab initio profile of each monitored torsion, was computed using each MM output geometry as a starting structure for a constrained geometry optimization, carried out keeping fixed the atomic coordinates of the four atoms defining that torsion. The ab initio conditions in the Jaguar calculations were exactly the same used for the charge analysis, i.e. HF method with 6-31G** basis set and default convergence criterion.

The PDB structures 1erm, 1ero and 1kds were carefully inspected with the program GRIN, implemented in the GRID software [36,37], to check the file against incidental errors that were subsequently manually corrected in MacroModel.

In the case of the 1kds complex, the monomer of the crystal structure with the best crystallographic properties[3] was selected for the studies reported here, because MacroModel 5.5 and 6.5 can manage molecules up to 5000 atoms. Hydrogen atoms were added on heteroatoms and on all the aromatic rings. Glutamic and aspartic residues were deprotonated while lysine and arginine residues were protonated. Crystal water molecules included in the calculations were: WAT 304, 341, 437, 438, 482 in the 1erm complex and WAT 400 and 401 in the 1kds complex.

All crystal structures were minimized to a derivative convergence of 10^{-3} kJ $Å^{-1}mol^{-1}$ using the Truncated Newton Conjugate Gradient (TNCG) minimization algorithm, the extended non-bonded treatment and the GB/SA water solvation model implemented in MacroModel, using the customized water.slv file (Table 4).

Because of the large number of atoms in the whole systems, a region of each enzyme centered on the inhibitor was selected, that included all the residues within 8 Å from the ligand. All calculations were performed on these internal subsets while the external residues were not considered in the minimizations and docking studies. Moreover, the side chains of some outstanding residues localized on the walls of the active site (namely: Lys67, Leu119, Gln120, Arg148, Tyr150, Asn152, Arg204, Ser212, Tyr221, Glu272, Asn289, Lys315, Thr316, Asn343, Asn346, Arg349 in the case of 1kds and Lys73, Glu104, Tyr105, Ser130, Asn132, Asn136, Glu166, Asn170, Lys234, Ser235, Glu239, Arg243, Arg273 in the case of 1erm and 1ero) and the crystal water molecules, when considered, were steadily minimized with the inhibitor to guarantee the complementarity between the surfaces of the two partners, while all the other atoms of the internal subset were restrained with a force constant of 400 kJ $Å^{-2}$ to avoid crystal structure rearrangement, even if their non–bonded interactions with all the relaxing atoms were calculated. Side chains of the active site residues (previously specified), water molecules and the respective inhibitors constitute the subsets considered in the RMSD calculations.

The Batchmin Monte Carlo Multiple Minimum methodology (MCMM command) was chosen to carry out flexible docking simulations performed by randomly rotating, in the range 30–120°, all the rotatable bonds of each inhibitor and the side chain of the catalytic serine. Because of the high number of rotational degrees of freedom, several consecutive runs (each one made of 9000 Monte Carlo steps) were repeated for each complex, using the SEED command. This command is used to start the Monte Carlo random number generator at a different point so that repeated MonteCarlo runs will give different results. Resulting geometries, combined, were minimized to a lower derivative convergence (10^{-3}kJ $Å^{-1}$ mol^{-1}).

Acknowledgements

Work supported by the Ministero dell'Istruzione dell'Università e della Ricerca (MIUR): program FIRB 2003, Protocol: RBNE034XSW_005. We would like to thank the "Centro Universitario per l'Informatica e la Telematica" of the University of Siena. M.B. thanks the Merk Research Laboratories (2004 Academic Development Program Chemistry Award).

[3] Amp–C complexes crystallize as homo-dimers (more than 6400 atoms), even though the enzyme works as monomer.

References

[1] C. Reading, M. Cole, Antimicrob. Agents Chemother. 11 (1977) 852–857.
[2] M.P. Groziak, Am. J. Ther. 8 (2001) 321–328.
[3] W. Yang, X. Gao, B. Wang, Med. Res. Rev. 3 (2003) 346–368.
[4] K.A. Keoler, G.E. Lienhard, Biochemistry 10 (1971) 2477–2483.
[5] O. Dobozy, I. Mite, I. Ferencz, V. Csanyl, Acta Biochim. Biophys. Acad. Sci. Hung. 6 (1971) 97–101.
[6] F. Morandi, E. Caselli, S. Morandi, P.J. Focia, J. Blazquez, B.K. Shoichet, F. Prati, J. Am. Chem. Soc. 125 (2003) 685–695.
[7] B.K. Shoichet, G.S. Weston, US Patent No., US 6,184,363 B1 of Feb 6, 2001.
[8] C. Therrien, R.C. Levesque, FEMS Microbiol. Rev. 24 (2000) 251–262.
[9] K. Bush, J.A. Jacoby, A.A. Medeiros, Antimicrob. Agents Chemother. 39 (1995) 1211–1233.
[10] F. Mohamadi, N.G.J. Richards, W.C. Guida, R. Liskamp, M. Lipton, C. Caufield, G. Chang, T. Hendrickson, W.C. Still, J. Comp. Chem. 11 (1990) 440–467.
[11] S.J. Weiner, P.A. Kollman, D.A. Case, U.C. Singh, C. Ghio, G. Alagona, S. Jr, P. Profeta, Weiner, J. Am. Chem. Soc. 106 (1984) 765–784.
[12] S.J. Weiner, P.A. Kollman, D.T. Nguyen, D.A. Case, J. Comp. Chem. 7 (1986) 230–252.
[13] D.Q. McDonald, W.C. Still, Tetrahedron Lett. 33 (1992) 7743–7746.
[14] S. Ness, R. Martin, A.M. Kindler, M. Paetzel, M. Gold, S.E. Jensen, J.B. Jones, N.C.J. Strynadka, Biochemistry 39 (2000) 5312–5321.
[15] R.A. Powers, B.K. Shoichet, J. Med. Chem. 45 (2002) 3222–3234.
[16] G.S. Weston, J. Blazquez, F. Baquero, B.K. Shoichet, J. Med. Chem. 41 (1998) 4577–4586.
[17] V. Martichonok, J.B. Jones, Bioorg. Med. Chem. 5 (1997) 679–684.
[18] V. Martichonok, J.B. Jones, J. Am. Chem. Soc. 118 (1996) 950–958.
[19] D. Tondi, R.A. Powers, E. Caselli, M.C. Negri, J. Blazquez, M.P. Costi, B.K. Shoichet, Chem. Biol. 8 (2001) 593–611.
[20] J.M. Goodman, I. Paterson, S.D. Kahn, Tetrahedron Lett. 28 (1987) 5209–5212.
[21] J.M. Goodman, S.D. Kahn, I. Paterson, J. Org. Chem. 55 (1990) 3295–3303.
[22] A. Vulpetti, M. Gardner, C. Gennari, A. Bernardi, J.M. Goodman, I. Paterson, J. Org. Chem. 58 (1993) 1711–1718.
[23] C. Gennari, E. Fioravanzo, A. Bernardi, A. Vulpetti, Tetrahedron 50 (1994) 8815–8826.
[24] J.J. James, A. Whiting, J. Chem. Soc., Perkin Trans. 2 (1996) 1861–1867.
[25] X. Chen, L. Bartolotti, K. Ishaq, A. Tropsha, J. Comp. Chem. 15 (1994) 333–345.
[26] D.S. Otkidach, I.V. Pletnev, J. Mol. Struct. THEOCHEM 536 (2001) 65–72.
[27] MacroModel BatchMin Reference Manual version 6.5, Appendix 3.
[28] J.J.P. Stewart, J. Comput. Aided Mol. Des. 4 (1990) 1–105.
[29] Jaguar ver. 4.1 Schrödinger Inc., Portland, OR, 19982001.
[30] W.C. Still, A. Tempczyk, R.C. Hawley, T. Hendrickson, J. Am. Chem. Soc. 112 (1990) 6127–6129.
[31] A. Tafi, A. van Almsick, F. Corelli, M. Crusco, K.E. Laumen, M.P. Schneider, M. Botta, J. Org. Chem. 65 (2000) 3659–3665.
[32] A. Tafi, F. Manetti, M. Botta, S. Casati, E. Santaniello, Tet.: Asymm. 15 (2004) 2345–2350.
[33] The software package InsightII was used to perform the graphics manipulations.
[34] Insight II, Accelrys Inc. 9685 Scranton Road, San Diego, CA 92121-3752, USA.
[35] M.J.S. Dewar, E.G. Zoebisch, E.F. Healy, J.J.P. Stewart, J. Am. Chem. Soc. 107 (1985) 3902–3909.
[36] P.J. Goodford, J. Med. Chem. 28 (1985) 849–857.
[37] P.J. Goodford, J. Chem. 10 (1996) 107–117.